Modeling Thermomechanical Behaviors of Shape Memory Polymer

Z. D. Wang, D. F. Li, Z. Y. Xiong, R. N. Chang

Institute of Engineering Mechanics, School of Civil Engineering, Beijing Jiao-Tong University, Beijing 100044, China

Received 9 August 2008; accepted 6 November 2008
DOI 10.1002/app.29656
Published online 23 March 2009 in Wiley InterScience (www.interscience.wiley.com).

ABSTRACT: The thermomechanical constitutive equations are critical for shape memory polymers (SMPs) in analyzing their shape, memory, and recovery responses under different constraints. In this study, a new physical-based, temperature and time-dependent constitutive model was proposed. The deformation mechanisms of this class of functional materials were explained, and the theoretical predicting values by different models were compared with available experimental results. © 2009 Wiley Periodicals, Inc. J Appl Polym Sci 113: 651–656, 2009

Key words: shape memory polymer; thermomechanical constitution; frozen fraction

INTRODUCTION

Shape memory polymers (SMPs) possess the ability to store and recover large strains by experiencing a prescribed thermomechanical cycle. The thermal-induced storage and recovery mechanisms have been described in molecular structure as shown in Figure 1.[1] A SMP consists of amorphous segments with an appropriate cross-linking density. As the temperature is higher than the switching transition temperature, T_{tran}, the amorphous segments are flexible, and the polymer is in the rubber state (initial state). More than several hundred percents of elastic strains can be performed through large-scale conformational changes. When keeping such deformation and cooling down the temperature well below T_{tran}, the amorphous segments are fixed and the large-scale conformational changes become impossible. The predeformed strain can be basically sustained even if the applied load is removed (temporary state). After reheating the temperatures to be above T_{tran}, the amorphous segments become flexible again. The permanent shape (initial state) is recovered because of the micro-Brownian thermal motion.

SMPs have many advantages over shape memory alloys and ceramics in easy processing, low density (1.0–1.3 g/cm^3), high shape recovery (maximum shape recovery ratio more than 400%), and low manufacturing cost. Their potential applications are receiving much attention. For example, the biodegradable SMPs are useful in medicine including wound sutures, filling, and sealing cranial aneurysms.[2–4] Continuous-fiber-reinforced shape memory composites have developed substantial interest in future deployable space-structure industry.[5–7] Several investigators have exploited the SMP-based MEMs with functions such as gripping or releasing therapeutic medical devices within blood vessels.[8,9]

The thermomechanical constitution is critical in predicting the deformation and recovery responses of SMPs under different constraints. Some works have been carried out in this field. For example, Bhattacharyya and Tobusi[10,11] proposed a rheological constitutive model, which did not consider the strain storage and recovery mechanisms. Rao[12] delineated the modeling of SMPs into four parts and addressed these parts separately by using a framework that was developed for studying the crystallization behavior of polymers.[13,14] Liu et al.[15] developed a small-strain constitutive model that seemed to be able to explain the thermomechanical testing results of SMPs. However, so far, the previous models are rate-independent. The frozen fractions of prestrain and thermal strain are not differentiated. Moreover, the applied mix-law is not suitable in predicting the equivalent Young's modulus of SMPs as considering the significant difference of Young's moduli in frozen and active states. In this study, a new thermomechanical model was proposed to avoid such deficiencies. The modeling results were verified by the available tests.

Correspondence to: Z. D. Wang (zhdwang@bjtu.edu.cn).
Contract grant sponsor: Natural Science Foundation of China; contract grant numbers: 10872025, 10502025.
Contract grant sponsor: Ministry of Education of the People's Republic of China (NECT).

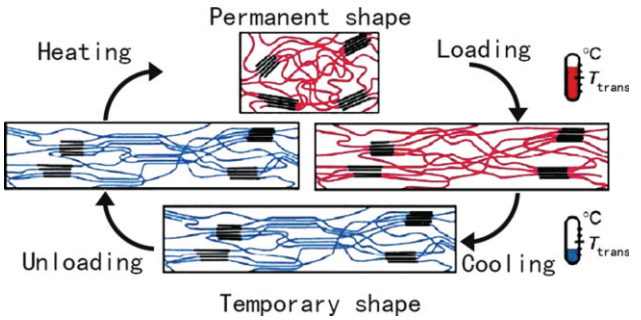

Figure 1 Schematic representation of the molecular mechanism about the thermal induced one-way shape memory effect. [Color figure can be viewed in the online issue, which is available at www.interscience.wiley.com.].

THERMOMECHANICAL CONSTITUTIVE MODEL

Frozen fraction

In a three-dimensional mode, the frozen fraction and the active fraction satisfy

$$\Phi_f(T) = \frac{V_f(T)}{V}, \quad \Phi_a(T) = \frac{V_a(T)}{V}, \quad \Phi_f(T) + \Phi_a(T) = 1, \tag{1}$$

where V is the total volume of the polymer, V_f the volume of the frozen phase, and V_a the volume of the active phase.

The shape memory and recovery characteristics are determined by the frozen volume fraction, which is a critical parameter. Liu et al.[15] assumed the frozen volume fraction as a phenomenological function of the temperature with two variables, c_f and n

$$\Phi_f = 1 - \frac{1}{1 + c_f(T_h - T)^n}, \tag{2}$$

where T_h is the predeformation temperature.

It is clear that there is a significant deficiency in eq. (2). The predeformation temperature is not a material variable. Different researchers gave different predeformation temperatures. For example, $T_h = T_{\text{tran}} + 20$ K in Liu et al.'s report. Tobushi et al.,[11] however, gave the relationship of $T_h = T_{\text{tran}} + 15$ K.

Considering the significant change of material's parameters during the glass change region, $T_l \le T \le T_h$, Tobushi et al.[11] simply assumed that all material parameters (e.g. Young's modulus, viscosity and yielding stress) could be generally expressed by an exponential function of the temperature

$$x = x_{\text{tran}} \exp\left[a\left(\frac{T_{\text{tran}}}{T} - 1\right)\right], \quad (T_l \le T \le T_h) \tag{3}$$

where x_{tran} is the value of the general material parameter x at $T = T_{\text{tran}}$, T_l is the strain storage temperature. It is clear that eq. (3) cannot give an accurate explanation about the shape memory and recovery characteristics of SMPs, and the predictive power is limited. Therefore, a more convinced and physical-based expression of the frozen fraction should be proposed.

Figure 2 shows the typical experimental results about the frozen strain of SMPs as a function of the temperature.[15] The frozen transition process focuses on a small transition zone. As the temperature is higher than a critical value, no frozen strain exists. When the temperature decreases to be lower than the critical value, the frozen strain increases quickly and soon goes to a saturation value close to the prestrain. This behavior is very similar to the crystallization process of semi-crystallization polymers. Hence, the crystallization theory can be applied to describe the frozen process of SMPs. According to the Avrami equation[16] modified by Ozawa,[17] the frozen process of SMPs is expressed as

$$\Phi_f(T, \beta) = \alpha \exp[-F(T)/\beta^n], \tag{4}$$

where α is the final frozen fraction. $F(T)$ is a function of the temperature, which can be normalized by the switching transition temperature T_{tran} as $F(T) = (T_{\text{tran}}/T)^m$, β, and n are the cooling rate and Avrami exponent, respectively.

Equation (4) indicates that the frozen process of SMPs is rate-dependent. Nonisothermal cooling will lead to lower temperature than isothermal cooling to receive the same frozen fraction. For isothermally increasing or decreasing the temperature, eq. (5) can be further simplified as

$$\Phi_f(T) = \alpha \exp[-K(T_{\text{tran}}/T)^m], \tag{5}$$

where $K = 1/\beta^n$ is a material's constant. As a type of polymers, the frozen deformation of SMPs is not an instantaneous response, but a time-consuming process. The transition temperatures should be

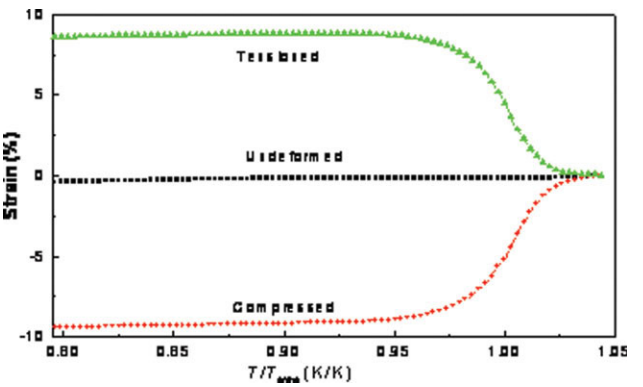

Figure 2 Testing results of the frozen strains as a function of the temperatures. [Color figure can be viewed in the online issue, which is available at www.interscience.wiley.com.].

different during the cooling and heating process. Therefore, the frozen fractions at a constant cooling/heating rate, β, can be expressed by eqs. (6) and (7), respectively:

$$\Phi_f(T) = \alpha \exp[-K(T_{\text{tran}}/T + \tau)^m], \quad (6)$$

$$\Phi_f(T) = \alpha \exp[-K(T_{\text{tran}}/T - \tau)^m], \quad (7)$$

where τ is the normalized retardant time, which is dependent on the cooling/heating rate as well as the microstructure of SMPs (e.g. cross-linking density).

Effective stiffness tensors

SMP can be regarded as a two-phase composite in the frozen transition region. The active phase and the frozen phase are matrix and reinforcement, respectively. Their volume fractions are temperature-dependent. With decreasing the temperature, the volume fraction of the matrix (active phase) is decreased and that of the reinforcement (frozen phase) is increased. Finally, the volume fraction of the frozen phase is much higher and nearly close to 100%. Hence, Mori-Tanaka approach[18] can be used to predict the effective elastic properties of SMPs as both matrix/reinforcement action and reinforcement/reinforcement action are considered in this model. Following this approach, the overall elastic-stiffness tensor of SMPs is

$$\tilde{\mathbf{L}} = \mathbf{L_a}\left(\mathbf{I} + \Phi_f \mathbf{A}\right)^{-1}, \quad (8)$$

$$\mathbf{A} = \{\mathbf{L_a} + (\mathbf{L_f} - \mathbf{L_a})\}\left[\Phi_f \mathbf{I} + (1 - \Phi_f)\mathbf{S}\right]^{-1}(\mathbf{L_a} - \mathbf{L_f}),$$

where the boldface terms indicate tensor quantities, $\mathbf{L_a}$ and $\mathbf{L_f}$ are, respectively, the stiffness tensors of the active phase and the frozen phase, $\mathbf{I}$ is identity tensor, $\mathbf{S}$ is Eshelby tensor.[19] For spherical effective particle and an isotropic matrix, the components of Eshelby tensor can be simplified as[20]

$$S_{1111} = S_{2222} = S_{3333} = \frac{7 - 5\nu}{15(1 - \nu)},$$

$$S_{1122} = S_{2233} = S_{3311} = S_{1133} = S_{2211} = S_{3322} = \frac{5\nu - 1}{15(1 - \nu)},$$

$$S_{1212} = S_{2323} = S_{3131} = \frac{4 - 5\nu}{15(1 - \nu)}, \quad (9)$$

where ν is Possion's ratio of the active phase. Here, both active and frozen phases were assumed to be isotropically thermoelastic, and the frozen phase was considered to be spheroids of identical shape, to be perfectly bonded to the active phase. It is therefore evident that the composite stiffness tensors in eqs. (8) and (9) are isotropic.

Thermomechanical constitution

The following relation can be received when a prestrain applied on SMPs in the frozen transition region

$$\begin{aligned}\varepsilon &= \varepsilon^M + \varepsilon^T \\ &= \Phi_f^M \varepsilon^M + \left(1 - \Phi_f^M\right)\varepsilon^M + \Phi_f^T \varepsilon^T + \left(1 - \Phi_f^T\right)\varepsilon^T, \end{aligned} \quad (10)$$

where ε^M and ε^T are the mechanical and thermal strains; Φ_f^M and Φ_f^T are the mechanical and thermal frozen fractions, which can be determined by eq. (6) or (7).

Although the frozen fraction of SMPs is commonly expressed by one variable, here, we prefer to differentiate the mechanical and thermal frozen fraction in eq. (10) by different variables. For a prescribed thermomechanical cycle, the mechanical prestrain is received at the temperature to be higher than T_{tran}, which can be frozen mostly at $T < T_{\text{tran}}$. The thermal strain, however, is accumulated during the whole thermomechanical process. The part of the thermal strain accumulated at $T > T_{\text{tran}}$ can be frozen mostly as the temperature decrease to be lower than T_{tran}, but the part of the thermal strain accumulated at $T < T_{\text{tran}}$ can hardly be frozen. Hence, the values of the mechanical and thermal frozen fractions at the same temperature are different. Moreover, the effects of the mechanical and thermal strains are different. The mechanical strain is much higher than the thermal strain and can be frozen mostly at $T < T_{\text{tran}}$, which determines the shape storage characteristics of SMPs. The thermal strain, however, mainly determines the instant recovery stress of SMPs during the shape recovery stage.

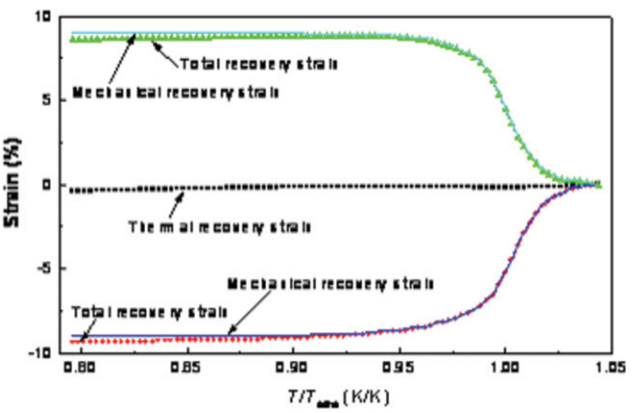

Figure 3 Total, thermal and mechanical recovery strains as a function of the temperatures. [Color figure can be viewed in the online issue, which is available at www.interscience.wiley.com.].

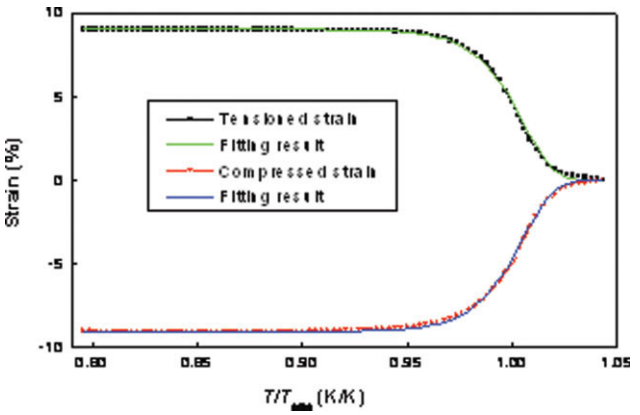

Figure 4 Mechanical tensioned and compressed frozen strains and the fitting results. [Color figure can be viewed in the online issue, which is available at www.interscience.wiley.com.].

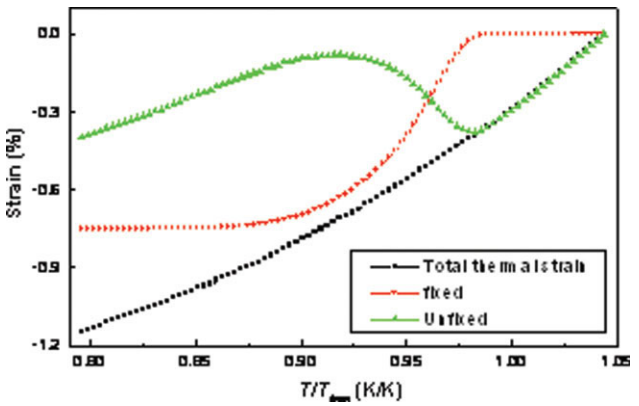

Figure 5 Total, fixed and unfixed thermal strains as a function of the temperatures. [Color figure can be viewed in the online issue, which is available at www.interscience.wiley.com.].

According to eq. (10), the overall constitutive equation of SMPs can be expressed as

$$\sigma = \tilde{\mathbf{L}}\left(\varepsilon - \varepsilon_f^M - \varepsilon_f^T\right) = \tilde{\mathbf{L}}\left[\varepsilon^{\text{pre}}\left(1 - \Phi_f^M\right) + \varepsilon^T\left(1 - \Phi_f^T\right)\right], \quad (11)$$

where variable $\tilde{\mathbf{L}}$ can be determined by eq. (8). ε^{pre} is the prestrain, which is equal to the mechanical strain, ε^M, as defined in eq. (10).

PARAMETERS DETERMINATION AND MODELING RESULTS

Here, the material parameters were determined according to the experimental results carried out by Liu et al.[15] The test specimens are one type of commercial thermoset epoxy systems, DP5.1 supplied by Composite Technology Development (CTD). The shape transition peak at approximately $T_{\text{tran}} = 343$ K, with a drop in storage modulus of approximately two orders of magnitude from $T_l = 273$ K to $T_h = 358$ K.

The theoretical frozen fraction is determined by the uniaxial free-strain recovery tests. According to the testing results shown in Figure 2, the mechanical frozen strain can be determined by the total recovery strain subtracted by the thermal recovery strain. Figure 3 presents the total and mechanical recovery strains at $\varepsilon^M = \pm 9.1\%$, and the thermal recovery strain. The mechanical frozen fraction, Φ_f^M, can be determined by the mechanical recovery strain divided by the prestrain and fitted by eq. (7). Figure 4 shows the fitting results. The mechanical fitting strain at a constant heating-rate can be expressed as

$$\Phi_f^M(T) = \varepsilon^M \alpha \exp\left[-K\left(T_g/T - \tau\right)^m\right]. \quad (12)$$

Table I listed the fitting results.

Comparing with the much higher mechanical prestrain, the effect of the thermal strain on the shape storage of SMPs is limited. However, the mechanical prestrain will be frozen mostly at $T < T_{\text{tran}}$ (see Fig. 3). The shape recovery stress during the heating process is significantly dependent on the thermal strain. Hence, the thermal strain of SMPs during the cooling/heating process must be considered independently. The total thermal strain was experimentally received. The frozen thermal strains at any temperature can be calculated by eq. (6) or (7), and the variables are listed in Table I. The unfrozen thermal

TABLE I
Estimation of Material Constants

A	K	τ	*m*
0.99	2.8	0.0192	75.5

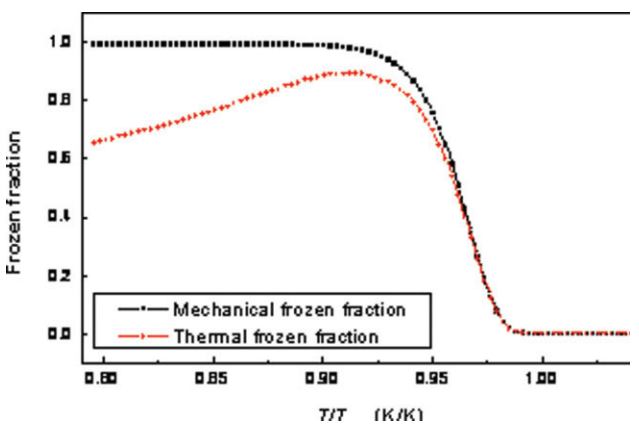

Figure 6 Mechanical and thermal frozen fractions as a function of the temperatures. [Color figure can be viewed in the online issue, which is available at www.interscience.wiley.com.].

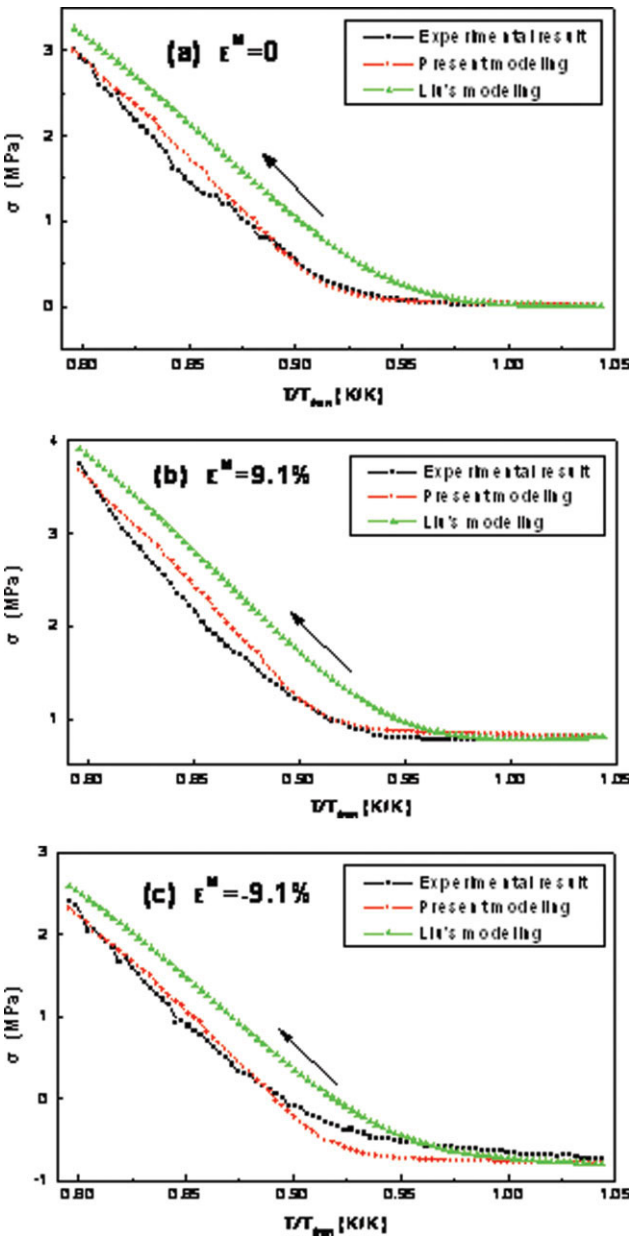

Figure 7 Stress responses of SMPs under different prestrain constraint conditions. [Color figure can be viewed in the online issue, which is available at www.interscience.wiley.com.].

strain is then determined by subtracting the frozen thermal strains from the total thermal strain. According to the fitting parameters listed in Table I, the effects of the temperature on total-, frozen-, and unfrozen-thermal strains are shown in Figure 5. As the temperature is higher than the frozen transition temperature, nearly no thermal strain is frozen, and the value of the unfrozen strain is close to that of the total thermal strain. As the temperature is in the frozen transition zone, both the existed and newly developed thermal strains will be frozen mostly. The increasing-rate of the frozen thermal strains is even higher than that of the total thermal strain. As the temperature decreases to be much lower than the frozen transition temperature, the frozen thermal strain will reach to a constant value, and the newly developed thermal strain cannot be frozen again.

Figure 6 provides the mechanical frozen fraction and thermal frozen fraction with decreasing the temperature. The mechanical frozen strain keeps nearly a constant value at $T < T_{tran}$ and cannot provide an initial shape recovery stress. The thermal strain, however, is changed during the whole shape recovery process. Therefore, the shape recovery stress is mainly determined by the thermal frozen strain.

Figures 7(a–c) show the experimental and fitting results of the stress responses of SMPs under different prestrain constraint conditions. The experiment was carried out by Liu et al.,[15] and their theoretical modeling results are also provided. The present predicting curves are not ideally smooth because of the effect of the thermal strain received from the experiment. However, the predicting results in this study are more close to the experimental values than that proposed by Liu et al. The critical point is that the frozen retardant time is considered in this model, but Liu et al. did not consider such factor. As comparing the heating/cooling tests respectively shown in Figures 2 and 7, it is clear that the transition temperatures for the same materials are different. Because the effect of the frozen retardant time was not introduced in Liu et al.'s model, the accuracy of their predictions is lower than that of this model.

CONCLUSIONS

The shape retaining and stress recovery response are critical for SMPs working as a kind of functional materials. In this study, a new constitutive model is proposed to predict the thermomechanical response of SMPs under different prestrain constraint conditions. The behaviors of the thermal-strain frozen fraction and mechanical-strain frozen fraction as a function of the temperature are compared. The frozen retardant time of SMPs is considered in the constitutive equations. The results show that the theoretical predictions can provide some reasonable explanations about the available testing results.

References

1. Lendlein, A.; Kelch, S. Angew Chem Int Ed Engl 2002, 41, 2034.
2. Murayama, Y.; Vinuela, F.; Tateshima, S.; et al. J Neurosurg 2001, 94, 454.
3. Robin, J.; Martinot, S.; Curtil, A.; Vedrinne, C.; Tronc, F. J Thorac Cardiovasc Surg 1998, 115, 898.
4. Wabers, H. D.; Hergenrother, R. W.; Coury, A. J.; Scooper, S. L. J Appl Biomater 1992, 3, 167.

5. Call, K.; Munshi, M. M.; Beavers, N. A.; et al. J Intel Mat Sys Struct 2000, 11, 877.
6. Tupper, M.; Gall, K.; Mikulas, M.; et al. IEEE 2001, 5, 2541.
7. Francis, W.; Lake, M. S.; Mallick, K. In Proceedings of AIAA; 2003, p 1496.
8. Gall, K.; Kreiner, P.; Turner, D.; et al. J Microelectromech Syst 2004, 13, 472.
9. Lee, A. P.; Northrup, M. A.; Ciarlo, D. R.; et al. U.S. Pat. 6,102,933 (2000).
10. Bhattacharyya, A.; Tobushi, H. Polym Eng Sci 2000, 40, 2498.
11. Tobushi, H.; Okumura, K.; Hashimoto, T.; et al. Mech Mater 2001, 33, 545.
12. Rao, I. J. In Proceedings of SPE-ANTEC; San Francisco, California, 2002.
13. Rao, I. J.; Rajagopal, K. R. Int J Solid Struct 2001, 38, 1149.
14. Rao, I. J.; Rajagopal, K. R. ZAMP 2002, 53, 365.
15. Liu, Y. P.; Gall, K.; Martin, L.; et al. Int J Plast 2006, 22, 279.
16. Avrami, M. J Chem Phys 1940, 8, 212.
17. Ozawa, T. Polymer 1971, 12, 150.
18. Mori, T.; Tanaka, K. Act Metall 1973, 21, 571.
19. Eshelby, J. D. Proc R Soc London Ser A 1957, 240, 367.
20. Eshelby, J. D. Proc R Soc London Ser A 1959, 252, 561.